

# Improving 2D-3D Registration Optimization Using Learned Prostate Motion Data

Tharindu De Silva<sup>1,2</sup>, Derek W. Cool<sup>1,3</sup>, Jing Yuan<sup>1</sup>, Cesare Romagnoli<sup>1,3</sup>,  
Aaron Fenster<sup>1,2,4</sup>, and Aaron D. Ward<sup>2,4</sup>

<sup>1</sup> Imaging Research Laboratories, Robarts Research Institute

<sup>2</sup> Biomedical Engineering Graduate Program, <sup>3</sup>Department of Medical Imaging

<sup>3</sup> Department of Medical Biophysics, The University of Western Ontario, Canada  
tdesilva@robarts.ca, aaron.ward@uwo.ca

**Abstract.** Prostate motion due to transrectal ultrasound (TRUS) probe pressure and patient movement causes target misalignments during 3D TRUS-guided biopsy. Several solutions have been proposed to perform 2D-3D registration for motion compensation. To improve registration accuracy and robustness, we developed and evaluated a registration algorithm whose optimization is based on learned prostate motion characteristics relative to different tracked probe positions and prostate sizes. We performed a principal component analysis of previously observed motions and utilized the principal directions to initialize Powell's direction set method during optimization. Compared with the standard initialization, our approach improved target registration error to  $2.53 \pm 1.25$  mm after registration. Multiple initializations along the major principal directions improved the robustness of the method at the cost of additional execution time of 1.5 s. With a total execution time of 3.2 s to perform motion compensation, this method is amenable to useful integration into a clinical 3D guided prostate biopsy workflow.

## 1 Introduction

Prostate biopsy is the clinical standard for cancer diagnosis and is typically performed under two-dimensional (2D) transrectal ultrasound (TRUS) for needle guidance. Unfortunately, most early stage prostate cancers are not visible on ultrasound, so the procedure is routinely performed in a systematic, but ultimately random fashion. The procedure suffers from high false negative rates due to the lack of visible targets [1]. Fusion of pre-biopsy MRI to 3D TRUS for targeted biopsy might improve cancer detection rates and volume of tumor sampled. Multiple 3D TRUS systems have been proposed [2,3,4,5] as well as some commercially available systems. In many MRI-3D TRUS fusion systems, the pre-biopsy MRI is registered to a static 3D scan acquired at the beginning of the procedure. Following the mapping of MRI lesions with the 3D TRUS image, each biopsy location is targeted using the live 2D TRUS image with real-time tracking of the probe orientation relative to the 3D TRUS volume. Any prostate motion due to TRUS probe pressure and/or patient movement breaks correspondence between the location of the targets identified in the baseline 3D TRUS

image and their actual physical location in the live 2D TRUS images. Therefore, accurate and fast registration to compensate for prostate motion during the procedure is important to successfully sample suspicious tumour locations.

In this work, we describe and evaluate a 2D-3D TRUS registration that incorporates knowledge of prostate motion characteristics into the optimization process in order to improve registration accuracy and robustness. Multiple algorithms have been proposed [4,6,3] to perform software-based motion compensation by registering intra-procedural TRUS images to an initially acquired 3D TRUS image. The system proposed in [3] used TRUS images acquired from a 3D TRUS probe to perform image-based tracking to compensate for motion. Xu et al. [4] performed the registration after initializing several previous 2D TRUS frames in a 3D coordinate system using the transformations provided by a magnetically tracked probe. We previously [6] proposed a 2D-3D registration method using an initialization provided by a mechanically-tracked probe. The registration needs to be performed in a transformation space of, at minimum, 6 dimensions (for rigid registration), and the non-convexity of the objective function in the search space can drive the optimizer to local optima. The methods in [4,6] rely on some initialization mechanism and then optimize an image-based, non-linear cost function using a local optimization technique whereas in [3] an initial global search mitigated local minima in the subsequent Powell-Brent search. While 2D-3D registration using a conventional real-time TRUS probe could be more challenging than 3D-3D registration [3] using a 3D TRUS probe, motion compensation with low inter-patient registration error variability and increased robustness is vital for successful clinical integration. In this work, we investigated whether, in a 2D-3D registration problem, the learned principal directions of motion induced at different probe positions for prostates with different sizes can be used to overcome local optima and drive the optimization to converge to the desired solution.

Statistical representations of high-dimensional transformations have been used to learn prostate deformations to improve MR-TRUS registration [7,8]. However, statistical analyses have been previously performed using finite element analysis (FEA)-simulated motion in 3D TRUS images [7] and phantoms [8] whereas this work utilized statistics of observed motion in actual prostate interventions. In this work, the principal components of observed prostate motion vectors were used to specify the initial optimization search directions. The rest of the paper describes our approach to learning of prostate motion characteristics and our adaptation of that learned statistical information to improve the search for the optimum of the cost function.

## 2 Methods

### 2.1 Data Acquisition

Using a mechanically-assisted biopsy system described in [2] we acquired 3D TRUS images with an end-firing 5-9 MHz TRUS transducer probe (Philips Medical Systems, Seattle, WA) during human clinical biopsy procedures. In addition

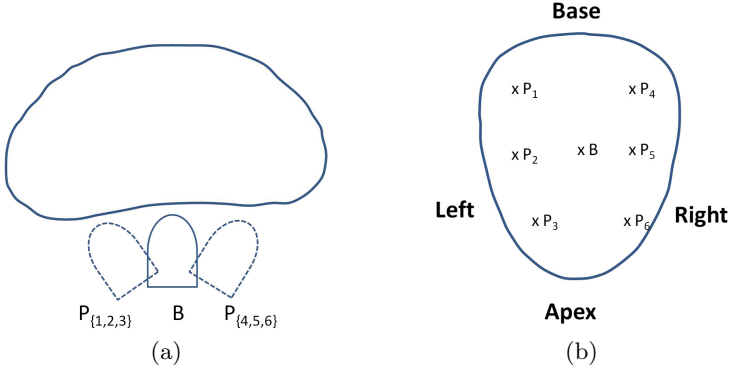


**Fig. 1.** Probe positions during image acquisition shown relative to (a) transverse view and (b) axial view (B - baseline, P - sextant locations)

to the baseline 3D TRUS image ( $I_B : \mathbb{R}^3 \rightarrow \mathbb{R}$ ) that would usually be acquired following the standard operating procedure for the system in [2], we acquired six other 3D TRUS images ( $I_{P_i} : \mathbb{R}^3 \rightarrow \mathbb{R}$  where  $i \in \{1, 2 \dots 6\}$ ) after positioning the TRUS probe at the corresponding standard sextant systematic biopsy locations. Figure 1 shows the relative bilateral sextant probe positions in base, mid and apex regions of the prostate. The mechanical encoders attached to the TRUS probe tracked the 3D position and orientation of the probe in real-time, which enabled the transformation of 3D volume to a common world coordinate system. Images were acquired from 29 patients following the protocol described above with 7 3D TRUS images per patient, for 203 images in total. During 2D-3D registration a transverse 2D slice ( $I_{P_i} : \mathbb{R}^2 \rightarrow \mathbb{R}$ ) was obtained from 3D TRUS images at each sextant probe position and registered to the baseline 3D image.

## 2.2 Principal Component Analysis (PCA) of Motion Vectors

Corresponding fiducial pairs of anatomically homologous points (corresponding, naturally-occurring micro-calcifications) were manually identified in 3D TRUS image pairs consisting of  $\{I_B, I_{P_i}\}$  for each patient. We denote the fiducials identified in the baseline image as  $f_B$  and those identified in the image with probe position  $i$  for that patient as  $f_{P_i}$ . For each patient  $j$ , we computed the optimal rigid alignment using the identified fiducials that defines the best six parameter rigid transformation vector  $\theta_{ij}^*$  out of all the possible rigid transformation vectors  $\theta_{ij}$  according to,

$$\theta_{ij}^* = \arg \min_{\theta_{ij}} \sum_{k=1}^K (f_{P_i}^k(\theta_{ij}(x, y, z)) - f_B^k(\Psi_{ij}(x, y, z)))^2, \quad (1)$$

where  $\Psi_{ij} : \mathbb{R}^3 \rightarrow \mathbb{R}^3$  is the transformation obtained from tracking the probe (which maps the 3D image to the world coordinate system) and  $K$  is the number of fiducial pairs identified per registration. Six such fiducial-based registrations

per patient were performed, one for each sextant location. A total of 1003 fiducial pairs were identified with an average of 6 fiducial pairs per registration. It is important to note that these fiducial pairs were identified only to measure and characterize prostate motion; *our registration algorithm is fully image-based and does not rely on the identification of fiducial landmarks.*

We conjectured that the motion characteristics of the prostate would depend on the position of the probe and its size, so we performed the PCA separately for each probe position and also separately for small (<40 cc) and large (>40 cc) prostates. In our data set of 29 patients, 18 were small prostates and 11 were large prostates. Each  $\theta_{ij}^*$  represents a point in the six-dimensional (6D) rigid transformation space that corresponds to the optimal rigid motion when the TRUS probe is at position  $i$ . For each probe position  $i$  and for prostates with similar sizes, we analysed the principal components of motion from the cloud of points in a 6D space consisting of observed prostate motions. We calculated a covariance matrix at a probe position  $i$  for each patient excluding that particular patient's motion  $\theta_{ij}^*$  according to the following equation.

$$COV = \frac{1}{N-1} \sum_{n=1}^{N-1} (\theta_{ij}^* - \bar{\theta}_i^*)^T (\theta_{ij}^* - \bar{\theta}_i^*), \quad (2)$$

where  $\bar{\theta}_i^*$  is the mean calculated excluding  $\theta_{ij}^*$  for the  $n$ th patient. The  $N$  of eq 2 would either be 11 or 18 depending the prostate size of that particular patient. The eigen vectors of  $COV$  yields a set of principal directions of motion  $\{U_1, U_2, \dots, U_6\}$  according to the variation of other observed motion vectors in that category.

### 2.3 Optimization Strategy

During registration, the normalized cross-correlation (NCC) is optimized as follows:

$$\arg \max_{\theta} NCC(I_{p_i}(\Psi_{2D-3D}(x, y, z)), I_B(\theta(x, y, z))). \quad (3)$$

where  $\Psi_{2D-3D}$  maps the 2D transverse slice  $I_{p_i}$  to the 3D world coordinate system and  $\theta$  is the registration transformation vector. We used Powell's method [9], which is a local optimizer that does not calculate the derivative of the function during optimization. For a  $D$ -dimensional quadratic function, line minimizations along  $D$  linearly independent, mutually conjugate directions will exactly find the function minimum. Powell's algorithm determines a set of such directions after initialization with the columns of any  $D \times D$  orthogonal matrix. For a non-convex function, which is the case for the above objective function in our context, repeated cycles of  $D$  line searches are done iteratively until convergence. Usually this initialization is performed using the column vectors of an identity matrix [9]. The vectors  $\{V_1, V_2, \dots, V_6\}$  obtained from an identity matrix would initially search along each translation and rotation direction in the six-dimensional rigid transformation space. However, these search directions may be suboptimal with respect to the avoidance of local optima.

Our approach is to use information obtained from the observed principal motion directions  $\{U_1, U_2, \dots, U_6\}$  to optimize the overall search strategy using Powell’s method. Experimentally, we found that the first three principal components of the motion vectors  $\{U_1, U_2, U_3\}$  explained 99% of the observed variance in our data set. Thus,  $\{U_1, U_2, U_3\}$  contain the directions in the transformation space corresponding to the *greatest amount* of inter-subject variability in the transformation for ideally accurate registration. It follows that  $\{U_4, U_5, U_6\}$  contain the directions in the transformation space corresponding to the *least amount* of inter-subject variability in the transformation for ideally accurate registration. Thus, the registration problem can be partitioned into two sub-problems: (1) registration by transformation along axes  $\{U_4, U_5, U_6\}$  (a relatively easier problem since the correct solution is very consistent across subjects), and (2) registration by transformation along axes  $\{U_1, U_2, U_3\}$  (a relatively more challenging problem since the correct solution has high inter-subject variability). Based on this observation, we designed a two-stage registration algorithm. In the first stage, we solve easier problem (1) by local optimization within the subspace  $\{U_4, U_5, U_6\}$  using Powell’s method to improve the initialization of the next stage. Then, we solve harder problem (2) by first performing an exhaustive local search on a grid oriented according to  $\{U_1, U_2, U_3\}$  (to mitigate local optima in this subspace where solutions have high inter-subject variability), and use the result to initialize a second Powell optimization within the space of the eigenvectors. The key insight behind this approach is that whereas an exhaustive 6D grid search is computationally expensive, it is feasible to mitigate local optima by performing an exhaustive search in the 3D space yielded by dimensionality reduction by PCA. The formal description of this algorithm is provided in algorithm below.

Step 1: Initialize the current position with  $\bar{\theta}_i^*$  of the patient for direction  $i$ .

Step 2: Perform Powell’s optimization along directions  $\{U_4, U_5, U_6\}$  corresponding to the directions with least inter-patient variability. Update current position  $\theta$ .

Step 3: Evaluate metric values on a grid of  $T_x \times T_y \times T_z$  points placed along directions  $\{U_1, U_2, U_3\}$  centred at the current position  $\theta$ . Update the current position with the best metric value location.

Step 4: Perform Powell’s method with the principal component vectors  $\{U_1, U_2, \dots, U_6\}$  as the basis.

For the experiments performed in this paper, the size of the grid in multiple metric evaluations was  $10 \times 7 \times 7$ . This method required minimization in 3 directions and 490 metric evaluations in addition to the conventional method. However, both the NCC calculation for a single image and independent metric evaluations can be performed in parallel to reduce the computation time.

## 2.4 Validation

For the 29 patients, we performed 174 registrations in total with 6 registrations per patient when the probe was positioned at each sextant biopsy location.

We validated the registrations using the manually identified fiducials for each image pair and calculated the root mean square (RMS) target registration error (TRE). We used leave-one-out cross-validation approach; fiducials in test images were excluded during PCA. To compare the results, we performed registrations using Powell’s method as in [9], henceforth referred to as the classical method, and using the updated version described in this paper and calculated the TREs separately for each method.

### 3 Results

Table 1 shows the RMS TREs and standard deviations (std) of errors before registration, after registration with the classical Powell’s method, after registration with the updated method, and fiducial registration errors (FRE). Figure 2 shows distributions of TREs before and after registration with the two methods. With the updated method, we observed a statistically significant difference in TRE (paired t-test rejected the null-hypothesis with  $p < 0.001$ ) compared to the classical method indicating an improvement in accuracy and robustness of the registration. After initializing with the learned principal directions of motion, the average number of iterations required for convergence decreased from 4.9 to 3.2. Using a GPU accelerated implementation for NCC calculation (NVIDIA GTX 580 GPU card and Intel Xeon 2.5 GHz processor), the updated method takes approximately an additional 1.5 s. However, multiple metric evaluations along the principal directions of motion can be executed in parallel to further reduce execution time during registration. Figure 3 contain five representative example images, depicting the visual alignment qualitatively before and after registration with the methods described in the paper.

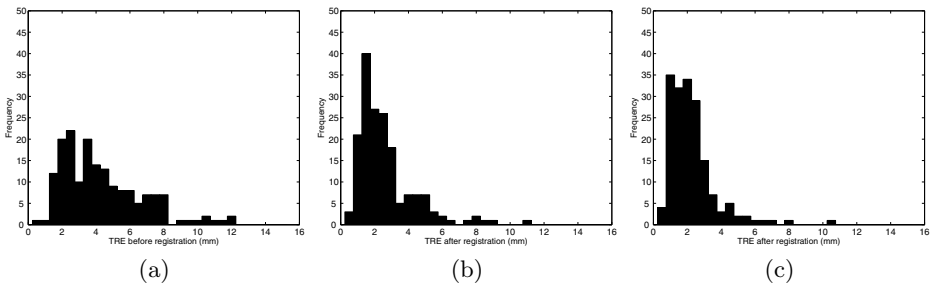


**Fig. 2.** TRE histograms (a) TRE before registration. (b) TRE after the classical method. (c) TRE after the updated method.

### 4 Discussion and Conclusions

Incorporation of learned prostate motions for optimizer search space improves 2D-3D TRUS registration. PCA yielded search directions consisting of rotation

**Table 1.** Comparisons of performance before, after registration and FRE

|                          | Before | Classical method | Our method | FRE  |
|--------------------------|--------|------------------|------------|------|
| RMS TRE (mm)             | 4.95   | 3.12             | 2.53       | 1.15 |
| std (mm)                 | 2.37   | 1.70             | 1.25       | 0.57 |
| Avg number of iterations | xx     | 4.9              | 3.2        | xx   |
| Execution time (s)       | xx     | 1.7              | 3.2        | xx   |

and translation along non-Euclidean basis vectors. The percentage of registrations with  $TRE > 5$  mm decreased from 9.2% to 2.3% with the updated method in comparison to the classical method, indicating improved robustness. The calculation of the best rigid transformations ( $\theta^*$ ) to characterize prostate motion is limited by the operator's ability to accurately identify and correspond fiducial locations. Since we considered the transformations given by the manually identified fiducials as the ground truth, fiducial localization error would challenge the registration algorithms in improving accuracy. Furthermore, any non-rigid deformation of the prostate would challenge our assumption of rigid motion. The ability of the registration to match the best rigid alignment calculated based on fiducials identified throughout the prostate could also be limited by the fact that we are restricted to using a single 2D slice during registration. In such a situation, non-rigid deformation might pose an additional challenge for the algorithm to estimate the overall rigid motion of the prostate by only using the image information in the 2D slice.

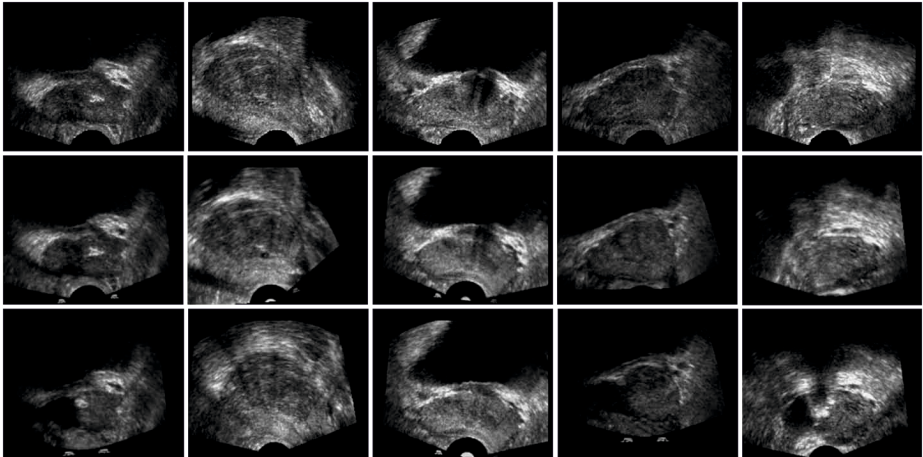


**Fig. 3.** Images before and after registration for 5 patients. Top row: extracted 2D images ( $I_{p_i}$ ). Middle row: corresponding frames from the registered  $I_B$ . Bottom row: corresponding frames before registration obtained from  $I_B$  after tracking the probe.

In this paper, we demonstrated that the learned prostate motion directions can be used to improve 2D-3D TRUS registration optimization, which may have application to MRI-3D TRUS fusion biopsy accuracy. Our results indicate that we can improve the accuracy and robustness of the algorithm, at the cost of 1-2 s of additional execution time.

**Acknowledgements.** The authors are grateful for the funding granted from the Canadian Institutes of Health Research (CIHR), the Ontario Institute of Cancer Research (OICR), and Cancer Care Ontario (CCO) for this work. A. Fenster holds a Canada Research Chair in Biomedical Engineering, and acknowledges the support of the Canada Research Chairs Program. A. D. Ward holds a Cancer Care Ontario Research Chair in Cancer Imaging.

## References

1. Leite, K.M., Camara-Lopes, L., Dall'Oglio, M., Cury, J., Antunes, A., Sañudo, A., Srougi, M.: Upgrading the gleason score in extended prostate biopsy: implications for treatment choice. *Int. J. Radiat. Oncol. Biol. Phys.* 73(2), 353–356 (2009)
2. Bax, J., Cool, D., Gardi, L., Knight, K., Smith, D., Montreuil, J., Sherebrin, S., Romagnoli, C., Fenster, A.: Mechanically assisted 3D ultrasound guided prostate biopsy system. *Medical Physics* 35(12), 5397–5410 (2008)
3. Baumann, M., Mozer, P., Daanen, V., Troccaz, J.: Prostate biopsy tracking with deformation estimation. *Medical Image Analysis* 16(3), 562–576 (2012)
4. Xu, S., Kruecker, J., Turkbey, B., Glossop, N., Singh, A.K., Choyke, P., Pinto, P., Wood, B.J.: Real-time MRI-TRUS fusion for guidance of targeted prostate biopsies. *Computer Aided Surgery* 13(5), 255–264 (2008)
5. Hadaschik, B.A., Kuru, T.H., et al.: A novel stereotactic prostate biopsy system integrating pre-interventional magnetic resonance imaging and live ultrasound fusion. *The Journal of Urology* 186(6), 2214–2220 (2011)
6. De Silva, T., Fenster, A., Cool, D.W., Gardi, L., Romagnoli, C., Samarabandu, J., Ward, A.D.: 2D-3D rigid registration to compensate for prostate motion during 3D TRUS-guided biopsy. *Medical Physics* 40(2), 022904 (2013)
7. Hu, Y., Ahmed, H.U., Taylor, Z., Allen, C., Emberton, M., Hawkes, D., Barratt, D.: Mr to ultrasound registration for image-guided prostate interventions. *Medical Image Analysis* 16(3), 687–703 (2012)
8. Mohamed, A., Davatzikos, C., Taylor, R.: A combined statistical and biomechanical model for estimation of intra-operative prostate deformation. In: Dohi, T., Kikinis, R. (eds.) *MICCAI 2002, Part II*. LNCS, vol. 2489, pp. 452–460. Springer, Heidelberg (2002)
9. Press, W.H., Teukolsky, S.A., Vetterling, W.T., Flannery, B.P.: *Numerical recipes in c: The art of scientific computing*. Cambridge U. Press, New York (1992)